PAPER

High-power narrow-band mode-locked sodium laser via double-stage sum-frequency generation

IOP Publishing | Astro Ltd Laser Physics

Laser Phys. **30** (2020) 085002 (7pp) https://doi.org/10.1088/1555-6611/ab9832

High-power narrow-band mode-locked sodium laser via double-stage sum-frequency generation

Ji Yao[1,2], Quan Zheng[1,3], Yuning Wang[3], Donghe Tian[3], Yi Yao[3], Xianghui Yang[3] and Wei Huang[1]

[1] Changchun Institute of Optics, Fine Mechanics and Physics, Chinese Academy of Sciences, Changchun Jilin 130033, People's Republic of China
[2] University of Chinese Academy of Sciences, Beijing 100190, People's Republic of China
[3] Changchun New Industries Optoelectronics Tech. Co., Ltd., 130012, Changchun, People's Republic of China

E-mail: zhengquan@cnilaser.com

Received 26 March 2020
Accepted for publication 5 May 2020
Published 14 July 2020

Abstract

A high-power, narrow-band, mode-locked sodium D_{2a} laser with a high sum-frequency efficiency is demonstrated by mixing actively mode-locked Nd:YAG 1064 and 1319 nm lasers in two LiB_3O_5 (LBO) crystals. The mode-locked lasers at 1064 nm (23.02 W output) and 1319 nm (17.98 W output) are generated from two diode, side-pumped, Nd:YAG, master oscillator power amplifier laser systems. A macro-micro pulse sodium beacon laser with a 30.2 W output power, 0.3 GHz (0.3 pm) linewidth, and a beam quality given by $M^2 = 1.23$ is obtained with a conversion efficiency of 73.6%. Compared with a single LBO crystal, the sum-frequency efficiency is enhanced by 14.5%. A laser coupled amplitude equation model, including the acousto-optic mode-locker, is applied for theoretical and numerical analyses of the sum-frequency conversion efficiency. The experimental results agree well with the theoretical calculations.

Keywords: actively mode-locked, sodium $D2_a$ laser, macro-micro pulse

(Some figures may appear in colour only in the online journal)

1. Introduction

Lasers at 589 nm, which are a coherent light source in resonance with sodium D_{2a} [1], can be used for sodium laser guide star adaptive optics (LGS AO) systems [2, 3]. When a 589 nm laser enters a sodium layer at an altitude of 90 km, a bright artificial star is produced, which is considered to be an ideal artificial star for AO systems to correct for the fast-changing aberrations caused by atmospheric turbulence [4]. First-generation sodium lasers were dye based [5], but these have been gradually phased out due to the sensitivity of their system, and problematic operation at remote astronomical observatories [6]. To date, two new sodium laser devices with a higher coupling efficiency, improved power output, and more reliable types of construction have been studied and tested, e.g. the sum-frequency generation (SFG) of all-solid-state Nd:YAG lasers [7–10], and a frequency doubling technology for a Raman fiber amplifier [11–14]. In addition, a 4.6 W continuous-wave (CW) mode-locked laser with an $M^2 = 1.12$ in a single-pass SFG in a PPMGO:SLT crystal has also been reported [15]. In another work, Taylor *et al* demonstrated a 50 W CW sodium beacon laser via frequency doubling from three coherentlycombined narrow-band Raman fiber amplifiers [16]. This laser was successfully applied to an AO system from the European Southern Observatory. Compared with a 589 nm CW laser, a microsecond pulse laser alleviates the stretching phenomenon in the LGS by providing a gateable pulse to reduce the impact of Rayleigh scattering from low-altitude atmosphere [17]. As a special kind of microsecond pulse sodium laser, the peak power for a macro-micro mode-locked pulse laser is N times higher than its non-mode-locked value, where N is determined by $N = \nu_{YAG}/(c/2l)$, with c being the speed of light, l being the

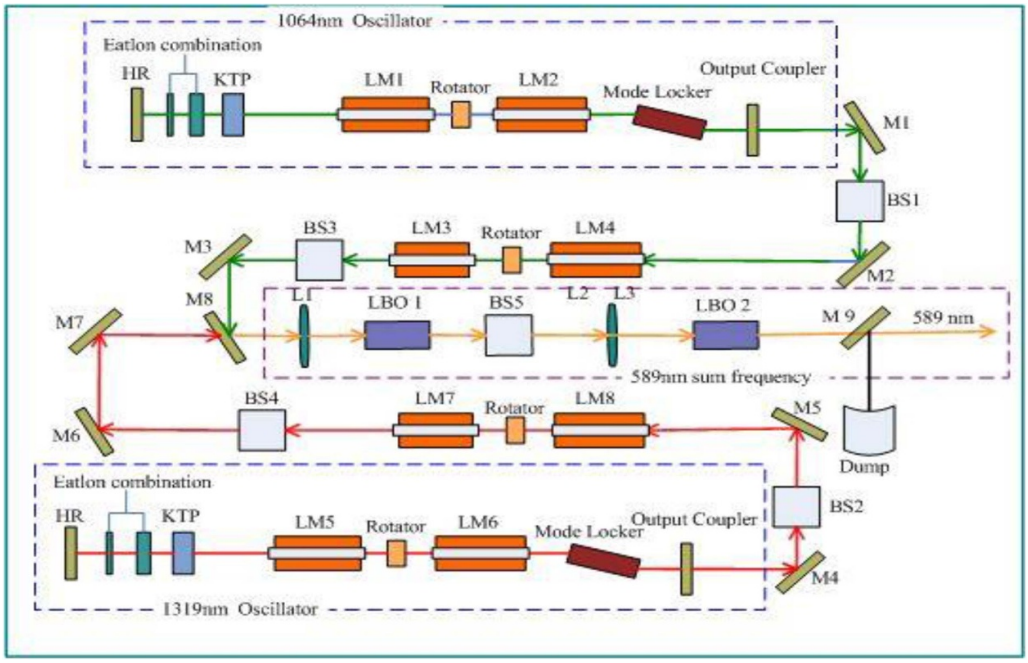

Figure 1. Schematic of the 589 nm laser system. BS1 and BS3, 1064 nm beam shaper; M1–M3, 45° high-reflection (HR) coating at 1064 nm; BS2 and BS4, 1319 nm beam shaper; M4–M7, 45° HR at 1319 nm; M8, 45° HR at 1064 nm and antireflection (AR) coating at 1319 nm; L1–L2, lens; LM1–LM8, laser modules; M9, AR-coated filter for 589 nm, 45° HR coating at 1319 and 1064 nm.

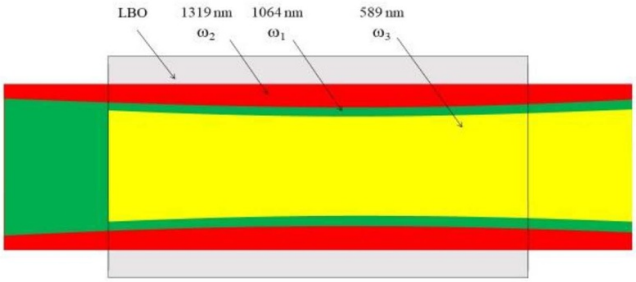

Figure 2. Process for the sum-frequency generation.

Table 1. Parameters for the fundamental frequency laser and Nd:YAG crystal.

Parameters	Value
P_{in} (1319)	17.96 W
P_{in} (1064)	23.02 W
Linewidth (1319)	0.8 GHz
Linewidth (1064)	0.4 GHz
d_{eff}	0.96 10^{-12} m V^{-1}
n_1	1.6054
n_2	1.6006
n_3	1.5963
$\Delta\theta$	56 mrad
ΔT	3.6 °C
L	30 mm
d	0.071796 mm
F	1. mm

cavity length, and ν_{YAG} being the spectral width of the fundamental laser. This result contributes to an increased SFG conversion efficiency and output power [18], while avoiding saturation of the sodium atoms, due to the chosen duty cycle being shorter than the lifetime of the sodium upper energy level [19].

In this paper, we report a high-power, narrow-band, mode-locked sodium D_{2a} resonance laser with a high sum-frequency efficiency. Two LiB3O5 (LBO) crystals are used in the SFG. Two mode-locked lasers with output powers of 23.02 and 17.96 W (power is measured by a FieldMax2 power meter, which is produce by Coherent Inc., and the power measurement error is ±1%) at 1064 and 1319 nm, respectively, are generated from two diode side-pumped Nd:YAG MOPA laser systems. Laser spiking is suppressed by inserting nonlinear crystals in the 1064 and 1319 nm oscillators. A sodium beacon laser at a 30.2 W output power is obtained, with a conversion efficiency of 73.6%, an increase of 14.5% over the use of LBO crystals. The beam quality factor is $M^2 = 1.23$, and the linewidth is 0.3 GHz (0.3 pm). To the best of the authors' knowledge, this is the highest output power and conversion efficiency reported for a macro-micro pulse laser at 589 nm. In comparison with traditional microsecond pulse lasers [20], although the output power of this paper is inferior, the regime of mode-locking affords two advantages. Firstly, the sum-frequency conversion efficiency of a macro-micro mode-locked pulse laser is much higher than that of the microsecond pulse, so the mode-locked pulse laser increases the output power more easily, as well as possessing a compact structure. Secondly, the peak intensity density of the sodium beacon with a mode-locking pulse laser is higher than that in a microsecond pulse laser [21, 22]. Thus, a brighter sodium

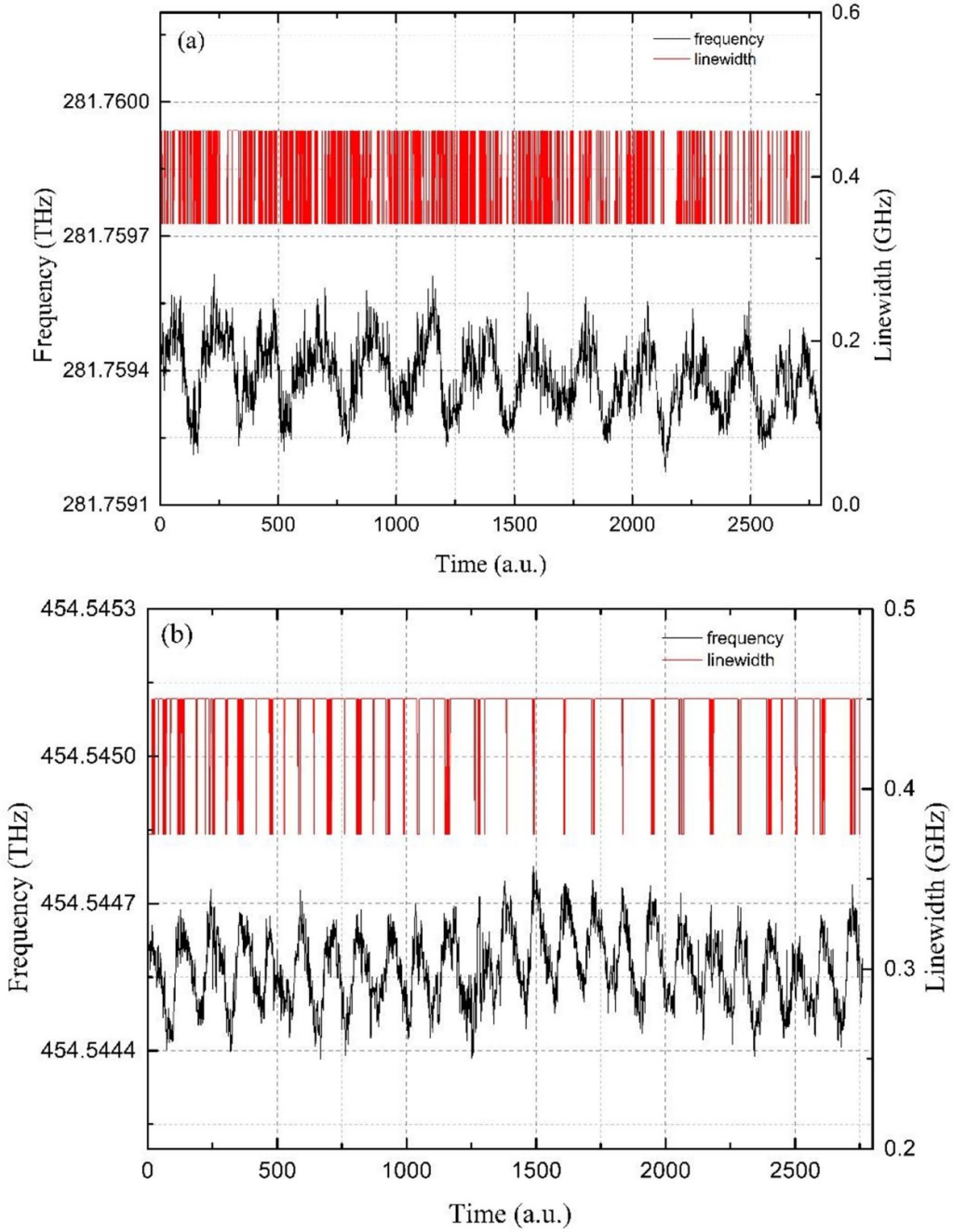

Figure 3. Frequency and linewidth at (a) 1064 and (b) 660 nm.

beacon will be generated by the mode-locking macro-micro pulse laser.

2. Experimental setup

A schematic of the experimental setup for the sodium laser is shown in figure 1. The 589 nm laser consists of three subsystems: a 1064 nm MOPA system, a 1319 nm MOPA system, and a double-stage SFG. The 1064 and 1319 nm MOPA systems are similar in their structure and features. The 1319 nm oscillator comprises two laser diode side-pumped Nd:YAG laser modules (LMs), a pair of Fabry–Perot (FP) etalons, a 90° quartz rotator (QR), an acousto-optic mode-locker, a nonlinear crystal, a high reflection mirror, and an output coupler. All of the laser modules share the same structure. Each laser module involves a Nd:YAG rod, which is threefold symmetrically side-pumped with three LD arrays at 808 nm. The Nd:YAG rods are 70 mm long and 3 mm in diameter, with an antireflection coating optimized for 1064 and 1319 nm. The pump power for each LD is 80 W, which increases the maximum input power by up to 240 W for each laser module, under a repetition rate of 500 Hz. By inserting a 90° QR at 1319 nm between the two laser modules, the depolarization effects caused by thermal birefringence are compensated for.

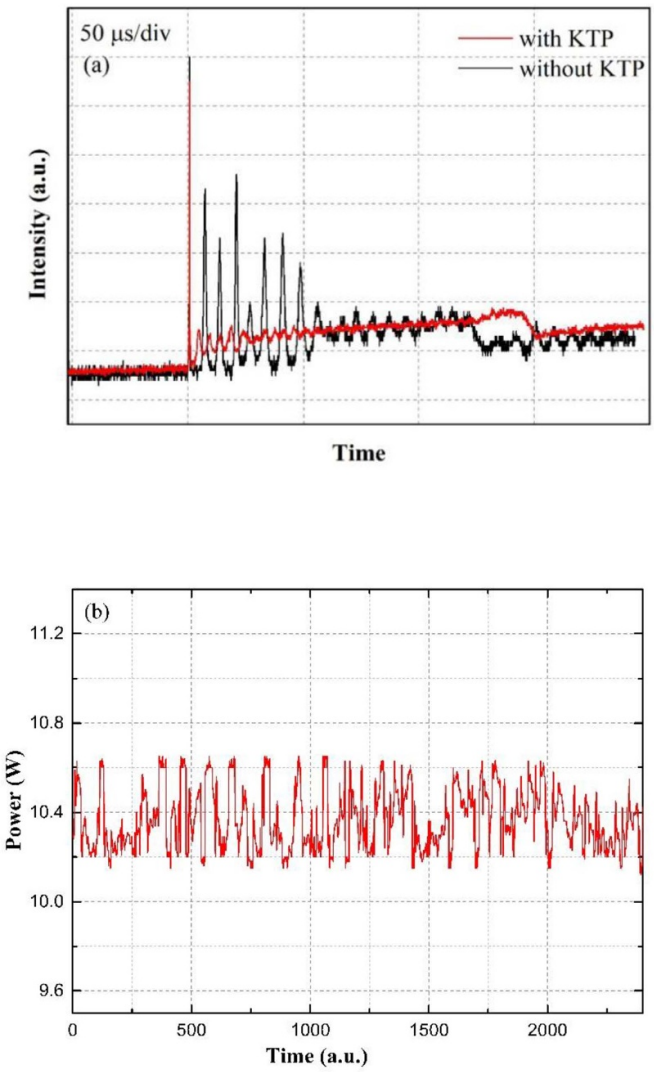

Figure 4. (a) Pulse profiles of the 1064 nm laser with and without the nonlinear crystal and (b) the output power of the 1064 nm laser.

Etalon combination is used to tune the wavelength with a narrow linewidth at 1319 nm by controlling the temperature of the FPs with a precision of 0.1 °C. The thicknesses of the etalons are 0.5 and 2.1 mm, and both have a reflection of 50%. A nonlinear crystal with an aperture size of 4 × 4 mm is used as the intracavity frequency doubler to suppress the relaxation oscillations. The cavity mode frequency is determined as f = c/2l, and the cavity length is controlled by moving the high-reflection mirrors, which are fixed to a high-precision translation stage. The cavity mode frequency is set to 100 MHz by adjusting the cavity length to 1.5 m. The resulting laser, with an output power of 8.01 W at 1319 nm, a linewidth of 0.8 GHz, and $M^2 = 1.21$, is obtained as the seed source.

The 1319 nm seed source is injected into a single-stage single-pass power amplifier (PA1), which is comprised of two laser modules, LM7 and LM8, and a 90° QR after the beam shapers (BS2). The QRs are used to reduce depolarization losses. The MOPA system at 1064 nm is similar to that at 1319 nm, except for the AR coatings and etalon thicknesses to narrow the linewidth. As a result, the output powers at 1064 and 1319 nm are 23.02 W ($M^2 = 1.21$, linewidth of 0.4 GHz) and 17.96 W ($M^2 = 1.23$, linewidth of 0.8 GHz), respectively, subsequent to single-pass amplification.

Table 2. Theoretical and experimental conversion efficiency of the 589 nm laser.

Theoretical Calculations		Experimental Results	
Type of sum-frequency	Without mode-locking	With mode-locking	With mode-locking
Single-pass LBO	20.1%	63.7%	59.1%
Double-stage LBO	33.4%	77.0%	73.6%

The output beams at 1064 and 1319 nm are well matched using a telescopic lens combination (BS3 and BS4), and are injected into the first LBO crystal to produce a 589 nm laser via the beam combiner M8, and a lens with a focal length of 150 mm. After the first SFG, the output beams are collimated and focused into the second LBO crystal with the BS5 and lens (L2). Two LBO crystals with a type-I phase matching both at a size of 7 × 7 × 30 mm are AR coated at 589, 1064, and 1319 nm on both faces. The crystals are placed in ovens to accurately control their temperatures with a precision of 0.1 °C. The double-stage SFG beam is split from the fundamental beams using a filter (M9), and is injected into the sodium cell to lock the wavelength of the SFG by tuning the 1064 nm wavelength.

3. Theoretical and numerical analyses

Theoretical and numerical analyses of the sum-frequency generation using two mode-locked lasers are presented. The SFG process is depicted in figure 2. Three electromagnetic waves satisfy the energy relationship for the frequencies $w_3 = w_1 + w_2$ (ω_m is the angular frequency) and the momentum relationship for the wave vectors $k_3 = k_1 + k_2$ (κ_m is the wave vector). The theory of SFG is well established, and presented in the Handbook [23], and the conversion efficiency for a high consumption is given by [24]:

$$\eta_{consum} = \tanh(L/l_m) \tag{1}$$

$$l_m = \left[\frac{1}{c^2}\left(\frac{w_2^2 w_3^2}{k_2 k_3}\right)^{1/2} d_{eff} E_0(w_1, 0)\right]^{-1} \tag{2}$$

where L is the crystal length and l_m is the interaction length, $d_{eff} = \frac{\chi_{effi}}{2} = a_i \cdot \frac{\chi}{2} : a_j a_k$ is the effective nonlinear coefficient, and $E_0(w_2, 0)$ are the initial electric fields for the fundamental laser frequencies. Due to imperfect phase matching, $\Delta k \neq 0$. Thus, the total theoretical conversion efficiency of the SFG is defined by:

$$\eta_{theory} = \eta_{consum} \times \eta_{angle} \times \eta_{tem} \tag{3}$$

where $\eta_{angle} = \mathrm{sinc}^2(2.78\theta_1 L/10\Delta\theta)$ is the influencing factor for the angle mismatch, $\Delta\theta = 56$ mrad is the acceptance

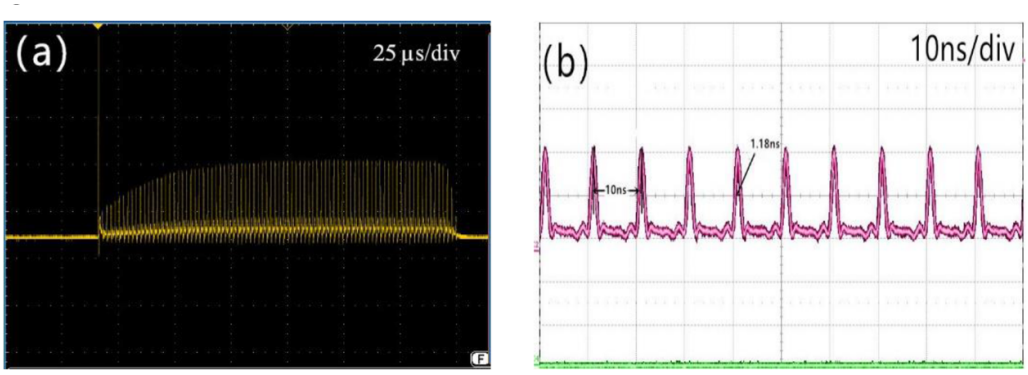

Figure 5. (a) Macro-micro and (b) micro pulse profiles of the mode-locked 589.159 nm laser.

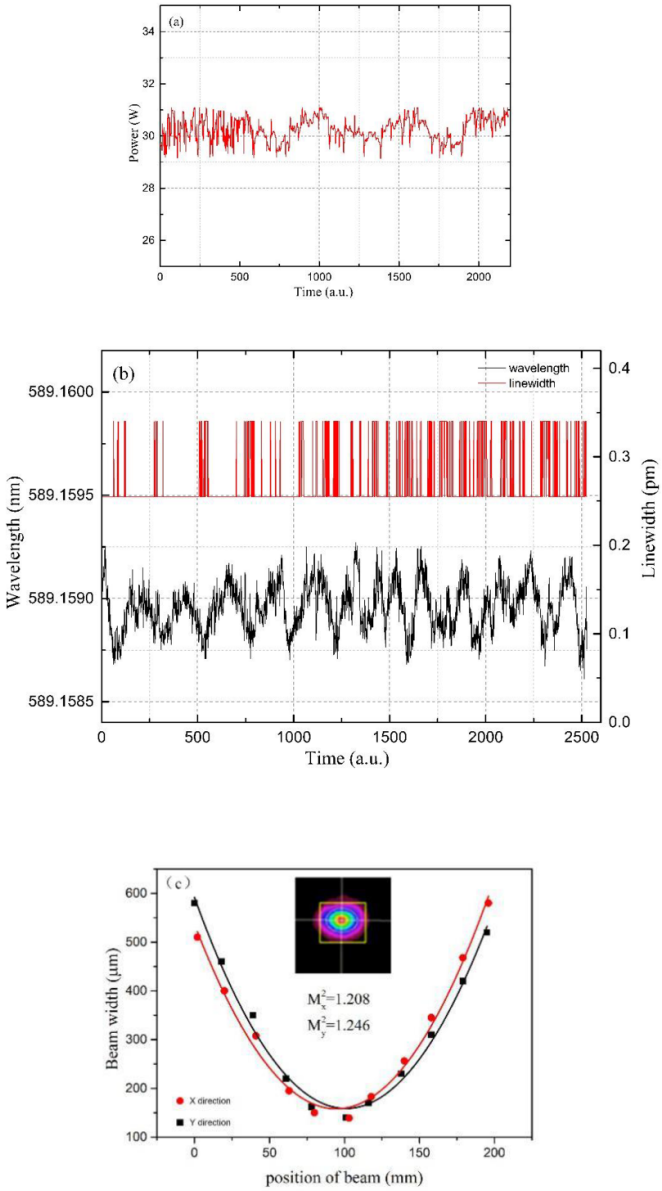

Figure 6. Parameters of the macro-micro pulse 589.159 nm laser using two crystals, showing its (a) power, (b) wavelength and linewidth, and (c) beam quality.

angle, $\theta_1 = 8\lambda_1/n_1\pi d$ is the divergence angle, d is the diameter of the incident laser at the crystal end face, $\eta_{tem} = sinc^2(2.78\alpha_1 L/10\Delta T)$ is the influencing factor of the temperature mismatch, $\alpha_1 = 0.5°\mathrm{C}$ is the absorption coefficient, and $\Delta T = 3.6°C$ is the acceptance temperature.

The peak power of the macro-micro pulse is N times the peak power without mode-locking; this is done to increase the sum-frequency conversion efficiency, where N is determined by [18]:

$$N = \frac{v_{YAG}}{(c/2l)}. \tag{4}$$

The linewidth of 1319 nm and 1064 nm is shown in figures 3(a) and (b). The linewidth at the second harmonic of 660 nm is measured using a wavelength meter, as 1319 nm is beyond the range of the equipment. By solving the coupled equations (1), (3), and (4), using the parameters of the fundamental lasers and Nd:YAG crystal listed in table 1, the theoretical single-pass SFG conversion efficiency of the AO mode-locked pulse laser is 62.7%, which is 3.1 times higher than its non-mode-locked value.

In order to increase the output power and conversion efficiency, the output lasers are collimated and focused into the second LBO crystal after passing through the first crystal. The theoretical and numerical analyses are similar to those for the single-pass SFG, unless the power densities of the incident lasers are different. The output power is 30.96 W after passing through the two LBO crystals. Compared with the single LBO crystal, the SFG efficiency increases by 12.8%.

4. Experimental results and discussion

In general, relaxation oscillations cause pulse-pumped solid-state lasers to have a low SFG efficiency. To improve the SFG efficiency, a nonlinear crystal is inserted into the fundamental laser to suppress its spiking behavior. The pulse profiles at 1064 nm are measured with and without the nonlinear crystal, as shown in figure 4(a). The relaxation oscillations of the lasers are significantly suppressed, and the output power at 1064 nm, as emitted from the oscillator, is shown in figure 4(b). The pulse profiles at 1319 nm are similar to those of the 1064 nm laser.

An acousto-optic mode-locker is inserted into the basic laser cavity to increase the output power and number of LGS photon returns. The macro-micro pulse profile of the AO mode-locker is 589.159 nm, and the duration of the microsecond pulse is 150 μs, as shown in figure 5(a). The macro pulse contains tens of thousands of micro pulses, resulting in a high peak power for the macro-micro pulse laser. The period and duration of the micro pulse is 10 and 1.18 ns, as shown in figure 5(b); this is chosen to be shorter than the lifetime of the sodium upper energy level (16 ns). Therefore, this duration limits the saturation of the sodium atoms. A digital signal delay device is applied to control the synchronization between the fundamental lasers by adjusting the delay times of the power supplies. The 589.159 nm laser, with an output power of 24.13 W, and a 58.9% SFG efficiency, is obtained by adjusting the delay between the 1064 and 1319 nm lasers. The experimental SFG efficiency is in excellent agreement with the theoretical calculations.

Subsequent to collimation and focusing, the laser output from the first LBO crystal is combined into the second LBO crystal. The average output power and linewidth of the 589 nm laser at a repetition rate of 500 Hz is measured to be 30.2 W (peak power is 1200 W, which is almost three times the peak power without mode-locking) and 0.3 GHz (0.3 pm), respectively, as shown in figures 6(a) and (b). The SFG efficiency is 73.6%, which is an improvement of 14.5% compared with a single crystal. The 589.159 nm laser beam quality factors are measured to be 1.227 ($M_x^2 = 1.208, M_y^2 = 1.246$) according to the beam quality analyzer, as shown in figure 6(c). The illustration shows that the 589.159 nm laser operates in a Gaussian mode, while the coherence relationship between the two stages is not obvious.

The results of the theoretical calculations and experiments are shown in table 2. It can be seen that the experimental results agree well with the theoretical calculations, and that the SFG efficiency value with mode-locking, after passing through two LBO crystals, is twice as high as its non-mode-locked value. To the best of our knowledge, a 30.2 W output power, and a conversion efficiency of 73.6% are the highest reported values for a macro-micro pulse laser at 589.159 nm.

5. Conclusion

We demonstrated a macro-micro mode-locked pulse laser generated using a double-stage single-pass SFG with two LBO crystals, based on actively mode-locked 1064 and 1319 nm lasers. The output power is 30.2 W, with an SFG efficiency of 73.6%, and a linewidth of 0.3 GHz (0.3 pm). The experimental sum-frequency conversion efficiency agrees well with the theoretical calculations.

Acknowledgments

This work is supported by Jilin Scientific and Technological Development Program (20170203013GX and 20180201117Gx), and Changchun New Industries Optoelectronics Tech. Co. Ltd (www.cnilaser.com).

References

[1] Hänsch T W, Shahin I S and Schawlow A L 1971 High-resolution saturation spectroscopy of the sodium D lines with a pulsed tunable dye laser *Phys. Rev. Lett.* **27** 707
[2] Calia D B *et al* 2004 Laser-guide-star-related activities at ESO *Proc. SPIE* **5490** 974–80
[3] Michael H 2018 Image registration for daylight adaptive optics *Opt. Lett.* **43** 1391
[4] Lu F, *et al* 2015 A Monte Carlo simulation for predicting photon return from sodium laser guide star *Proc. SPIE* **9678** 96781B
[5] Kanz V K 1995 Sodium beacon laser system for the Lick observatory *Proc. SPIE* **2534** 15935

[6] Roberts J E *et al* 2008 Facilitizing the Palomar AO laser guide star system *Proc. SPIE - Int. Soc. Opt. Eng.* **7015** 70152S
[7] Lu Y H, Xie G, Zhang L, Fan G-B, Pang Y, Li N, Wei B, Gao S-X, Zhang W and Tang C 2015 High-energy all-solid-state sodium beacon laser with line width of 0.6 GHz *Appl. Phys.* B **117** 253–9
[8] Peng-Yuan W *et al* 2014 33 W quasi-continuous-wave narrow-band sodium D2a laser by sum-frequency generation in LBO *Chin. Phys.* B **23** 094208
[9] Bian Q *et al* 2016 High-power QCW microsecond-pulse solid-state sodium beacon laser with spiking suppression and D_2b re-pumping *Opt. Lett.* **41** 1732
[10] Lu Y, *et al* 2017 Tunable line width all solid state double spectral line sodium beacon laser *Proc. SPIE* **2017** 10436
[11] Dong J, Zhang L, Cui S, Fan T, Dong J and Feng Y 2017 Sodium guide star laser pulsed at Larmor frequency *Opt. Lett.* **42** 4351–4
[12] Zhang L, Yuan Y, Liu Y, Wang J, Hu J, Lu X, Feng Y and Zhu S 2013 589 nm laser generation by frequency doubling of a single-frequency Raman fiber amplifier in PPSLT *Appl. Opt.* **52** 1636
[13] Surin A A, Borisenko T E and Larin S V 2016 Generation of 14??W at 589??nm by frequency doubling of high-power CW linearly polarized Raman fiber laser radiation in MgO: sPPLTcrystal *Opt. Lett.* **41** 2644
[14] Liu Y, Liu Z, Cong Z, Men S, Rao H, Xia J, Zhang S and Zhang H 2016 Quasi-continuous-wave 589-nm radiation based on intracavity frequency-doubled Nd: GGG/BaWO4Raman laser *Opt. Laser Technol.* **81** 184–8
[15] Saito N, Akagawa K, Ito M, Takazawa A, Hayano Y, Saito Y, Ito M, Takami H, Iye M and Wada S 2007 Sodium D-2 resonance radiation in single-pass sum-frequency generation with actively mode-locked Nd: YAG lasers *Opt. Lett.* **32** 1965–7
[16] Feng Y, Taylor L R and Calia D B 2009 25 W Raman-fiber-amplifier-based 589 nm laser for laser guide star *Opt. Express* **17** 19021–6
[17] Bradley L C 1992 Pulse-train excitation of sodium for use as a synthetic beacon *J. Opt. Soc. Am.* B **9** 1931–44
[18] Velur V, *et al* 2004 Implementation of the Chicago sum frequency laser at Palomar laser guide star test bed *Proc. SPIE* **2004** 5490
[19] Kibblewhite E J *et al* 1998 Performance of ChAOS on the Apache Point Observatory's 3.5-m telescope *Proc. SPIE* **3353** 300–9
[20] Bian Q, Bo Y, Zuo J-W, Feng L, Gao H-W, Yuan L, Cui D-F, Peng Q-J, Chen H-B and Xu Z-Y 2020 High-repetition-rate 100 W level sodium beacon laser for a multi-conjugate adaptive optics system *Opt. Lett.* **45** 1818–21
[21] Jie L 2018 Research on the compensation of laser launch optics to improve the performance of the LGS spot *Appl. Opt.* **57** 648
[22] Jin K *et al* 2014 Coupling efficiency measurements for long-pulsed solid sodium laser based on measured sodium profile data *Proc. SPIE* **9148** 91483L
[23] Dmitriev V G, Gurzadyan G G and Nikogosyan D N 1999 *Handbook of Nonlinear Optical Crystals/. Handbook of Nonlinear Optical Crystals* (Berlin: Springer)
[24] Boyd G D and Kleinman D A 1968 Parametric interaction of focused gaussian light beams *J. Phys. D: Appl. Phys.* **39** 3597–0